New Journal of Physics
The open access journal at the forefront of physics
Deutsche Physikalische Gesellschaft DPG | IOP Institute of Physics

Silicene on metal and metallized surfaces: *ab initio* studies

Paul Pflugradt, Lars Matthes and Friedhelm Bechstedt
Institut für Festkörpertheorie und -optik, Friedrich-Schiller-Universität and European Theoretical Spectroscopy Facility (ETSF), Max-Wien-Platz 1, D-07743 Jena, Germany
E-mail: paul.pflugradt@uni-jena.de

Received 27 March 2014, revised 8 May 2014
Accepted for publication 12 May 2014
Published 8 July 2014
New Journal of Physics **16** (2014) 075004
doi:10.1088/1367-2630/16/7/075004

Abstract
The deposition of silicene on several metals is investigated. For fcc crystals the (111) surfaces while for hexagonal ones the (0001) surfaces are used. The Ca (111)1 × 1 substrate is found to be the most promising candidate. The silicene adsorption on Ca-functionalized Si(111)1 × 1 and 2 × 1 surfaces is also studied. The 1 × 1 substrates lead to overlayer silicene with hexagonal symmetry and Dirac cones. However, the Dirac points are below the Fermi level, and small energy gaps are opened. In the case of 2 × 1 surfaces, strong lattice relaxation occurs. Only rudiments of conical linear bands remain visible.

Keywords: silicene, metal substrate, calcium, Dirac cone

1. Introduction

Silicon (Si) is the most important semiconductor because of its wide usage in electronic, optoelectronic and photovoltaic devices. Silicene, the two-dimensional (2D) silicon allotrope with honeycomb symmetry, has recently attracted wide attention due to its graphene-like electronic structure including the presence of Dirac cones near the Fermi level [1–4]. Theory predicts its stability in a low-buckled phase [3]. Moreover, because of its chemical nature it is compatible with Si-based electronics.

In contrast to graphene, which also arranges in a three-dimensional system, the sheet crystal graphite, for silicene no equivalent system is known. Therefore, silicene has to be

prepared by a certain epitaxial technique. Indeed, recent experiments show that epitaxial silicene, or more precisely silicene-like adsorbate layers, can be successfully grown on some metal or halfmetal substrates, such as Ag [5–8], Ir [9] and ZrB_2 [10]. However, because of the strong adsorbate–substrate interaction the occurrence of Si-derived Dirac cones is controversially discussed in the literature [11–17]. One alternative seems to be the epitaxial growth on non-metallic substrates with a reduced adsorbate–substrate interaction [18–20].

In this paper we simulate silicene deposition on metal substrates or on a metallic layer atop silicon. After the description of the methods in section 2, we summarize the results of a screening of the chosen metal surfaces with a hexagonal geometry in section 3. Since calcium (Ca) appears to be a promising candidate for a metal substrate, we also study thin Ca overlayers on Si(111) substrates in section 4.

2. Theoretical and numerical methods

The search for suitable substrates is driven by the calculation of atomic geometries, total energies, and electronic structures. All calculations are based on the density functional theory (DFT) as implemented in the Vienna *ab initio* Simulation Package (VASP) [21]. The 3*s* and 3*p* electrons of Si and the 4*s* electrons of Ca, the favored metal, are included in the simulation as valence electrons. The one-particle wave functions are expanded into plane waves up to a cutoff energy of 350 eV. The projector-augmented-wave (PAW) method [22] is applied to generate the pseudopotentials and describe the electronic states in the PAW spheres. Exchange and correlation are simulated in the framework of a density functional including van der Waals (vdW) interaction according to Dion *et al* [23] and implemented by Klimeš *et al* [24]. Dense **k**-point meshes [25] are applied to converge the total energies down to deviations smaller than 1 meV/atom and forces below 1 meV/Å. The resulting cubic lattice constant of diamond Si is $a_0 = 5.45$ Å and of the fcc metal Ca $a_0 = 5.54$ Å. The experimental values are $a_0 = 5.43$ Å and 5.58 Å, respectively [26].

The various surfaces are simulated by using symmetric slabs. For investigation of the silicon substrate system, slabs of 18 Si layers are used. For all metallic systems slabs with nine atomic layers are chosen. Because of periodic boundary conditions, we chose a vacuum region between the top layer of a slab and the bottom layer of the slab above, to separate surfaces. This vacuum region is fixed at 15 Å. The Brillouin zone (BZ) of a given repeated slab system is sampled by a $32 \times 32 \times 1$ ($16 \times 32 \times 1$) mesh for a 1×1 (2×1) reconstructed surface. For larger lateral unit cells we use an $8 \times 8 \times 1$ mesh [25]. For freestanding silicene the resulting lateral 2D lattice constant is $a = 3.86$ Å, while the vertical buckling of such a silicene sheet amounts to $\Delta = 0.48$ Å. These values agree with other vdW-DFT calculations [18]. The Fermi velocity for this silicene is $0.48{\times}10^6$ m s^{-1}. Quasiparticle corrections may increase this value by about 50% [27, 28] but should not considered here.

3. Screening of metal surfaces

We search for a metallic surface that may be suitable for the silicene epitaxy. We chose to investigate several elemental metals with nuclear number $Z < 90$ from the periodic table (see figure 1). We exclude the rare earths and actinides. We focus the search on fcc metals with (111) surfaces and hcp metals with [0001] orientation because of their hexagonal symmetry.

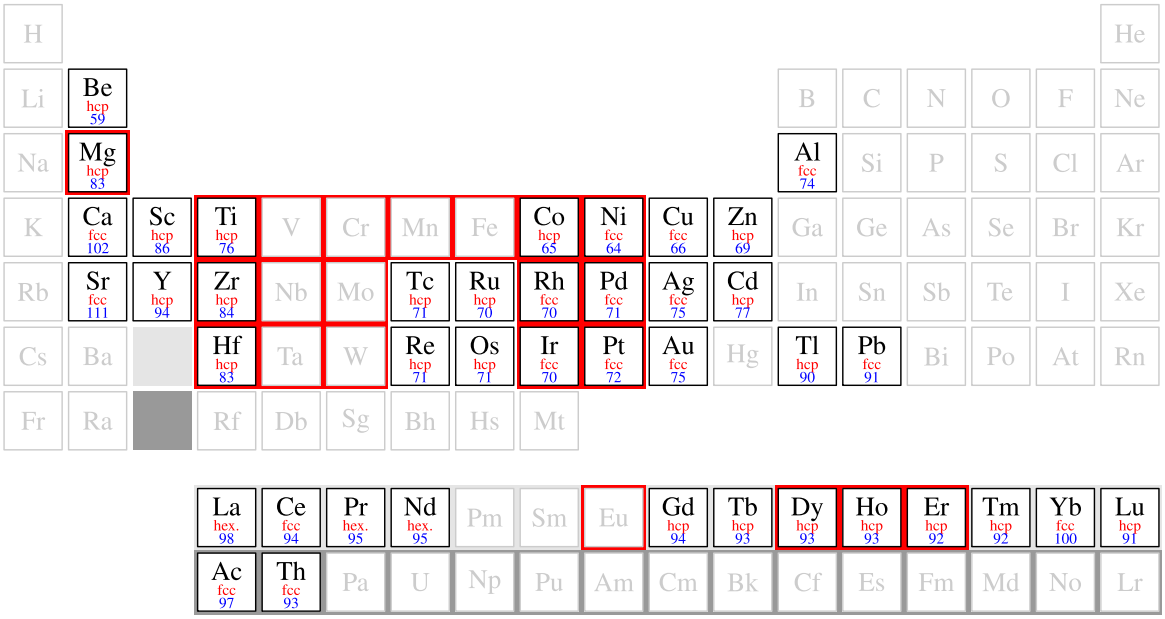

Figure 1. Periodic table. The metals with fcc and hexagonal structure are indicated. The corresponding (111) or (0001) surfaces have hexagonal symmetry. The crystal structure is indicated (in red) [26], while the relative lateral lattice constant compared to that of silicene is given as a (blue) number in per cent. The elements in red squares form silicides [29].

Mostly all metals that form silicides (see e.g. [29]), are excluded, because a strong metal–silicene interaction is expected. The corresponding relation of the surface lattice constant to the silicene value (see figure 1) helps to find reasonable coincidence lattices [30]. By allowing rotations around the surface normal and enlargements of the unit cells of silicene and the metal surface, the $(n \times m)R\varphi^0$ silicene layer is related coincidentally to the $(n' \times m')R\varphi'^0$ Bravais lattice of the metal surface. Here, we use the Wood notation [30]. The lateral lattice constants of the metal surfaces are derived from the experimental lattice constants of the bulk systems [26], while the DFT–vdW value $a = 3.86$ Å is used for silicene. For further investigations of the silicene/metal combinations, a single coincidence lattice with a small lateral lattice mismatch as well as a small overall cell size is selected from all possible coincidence lattices. We know that freestanding silicene can be biaxially strained up to ± 4 % without opening gaps between the Dirac cones [31]. This strain is not exceeded for any studied silicene/metal combination. Silver is excluded from our search, since the silicene deposition on it is thoroughly discussed [11–16, 32]. However, we followed the tendency for small coincidence lattices, found in the silicene/silver case, as a criterion for favorable combinations of translational symmetries [32].

As a result of the described screening procedure we found promising combinations of silicene monolayers (MLs) on a metal for 1×1 silicene on Ca(111)1×1, $(\sqrt{7} \times \sqrt{7})R19.1°$ on $(\sqrt{13} \times \sqrt{13})R13.8°$ Ti(0001), 3×3 on $(\sqrt{13} \times \sqrt{13})R13.9°$ Zr(0001) or Cd(0001), 2×2 on 3×3 Ru(0001), and 2×2 on $(\sqrt{7} \times \sqrt{7})R19.1°$ Au(111). In the case of Zn(0001) we used an oblique coincidence lattice $(\sqrt{7} \times \sqrt{13})R19.1°$ on $(\sqrt{13} \times \sqrt{28})R13.9°$. As the latteral lattice

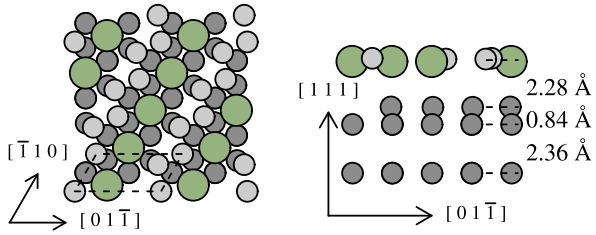

Figure 2. Top (left panel) and side (right panel) views of a triple-bond Si(111)2 × 1 surface covered by 0.5 ML Ca. The Ca (Si) atoms are shown as green (grey) dots. The substrate Si layers are darkened. The dashed lines illustrate the lateral surface unit cell. The numbers give the characteristic vertical distances.

constants of Ti and Au are very close to that of Ag, coincidence lattices have been studied, which have also been observed experimentally for silicene MLs on Ag(111) (see [32] and references therein).

Despite the fact that Ti and Zr may form a silicide (see figure 1) we have studied the seven suggested adsorbate systems by means of minimization of the total energy with respect to the atomic positions for different starting configurations of silicene relative to the metal surface. For Si atoms of the silicene overlayer we found a strong tendency to fill high-symmetry sites on the metallic surface. As a consequence, even for metals where a very weak interaction was anticipated, namely Zn and Cd, the silicene sheet adapts to the surface structure. Because of the lattice match, only for the 1 × 1 surface of Ca is the silicene 1 × 1 starting geometry not destroyed by atomic relaxation.

Consequently the resulting band structures only show silicene-derived Dirac cones in the case of deposition on Ca(111). Despite the less symmetric silicene adsorbate layer, we observe indications for Dirac cones, or more precisely, conical linear bands, also for Au, Cd and Zn substrates. However, similarly to the findings for 3 × 3 silicene on 4 × 4 Ag(111), the corresponding band states are derived from hybridized metal states [13–16, 32]. The most promising metal substrate seems to be the Ca(111) surface that will be investigated in detail in the next section.

4. Calcium and Ca-functionalized surfaces

4.1. Possible Ca-derived surfaces

In the previous section we found the possible stabilization of a silicene 1 × 1 overlayer with a lattice constant a = 3.86 Å on a flat Ca(111)1 × 1 surface with a lattice constant a = 3.92 Å and a tensile biaxial strain of 1.5% in the silicene adsorbate layer. We know that a Si(111)1 × 1 surface is almost lattice-matched with the silicene. However, the clean Si(111) surface cannot be used to grow silicene. Rather, passivation is needed [18]. Indeed, experimental studies showed that the adsorption of Ca atoms leads to a stable and passivated surface, but results in a 2 × 1 reconstruction, i.e., to Ca/Si(111)2 × 1 with a rectangular or oblique 2D Bravais lattice and 0.5 ML of Ca [33, 34]. The top and side views of this adsorbate system are illustrated in figure 2.

The result of an total-energy optimization confirms that this 2 × 1 Ca-covered surface phase is formed by π-bonded Seiwatz Si chains[30]. As divalent metal atoms, the Ca atoms are

bonded to two Si atoms. The Ca atoms fill the trenches between the π-bonded zig-zag chains of Si atoms, positioned on hollow sites of the silicon layer beneath. This surface is, however, not stable against higher temperatures and some annealing procedures [35]. Nevertheless, according to the total-energy calculation it forms a metastable surface, at least at low temperatures. In order to account for fluctuating Ca coverages and surface translational symmetries in growing an overlayer, we investigate several Ca/Si adsorbates. We use three 2 × 1 Si(111) reconstructions with 0.5, 1 and 1.5 ML of Ca and the 1 × 1 Si(111) surface with 1 ML of Ca. Together with silicene on Ca(111)1 × 1, silicene on five Ca-derived substrates are studied.

4.2. Silicene overlayers: structure and energetics

The optimized geometries of silicene on the most stable Ca(111)1 × 1 or Ca-covered Si(111) surfaces are presented in figure 3. Silicene on clean Ca(111)1 × 1 substrate (figure 3(a)) as well as silicene on the Ca(1.0ML)-functionalized Si(111)1 × 1 surface (figure 3(c)) exhibit perfect hexagonal symmetries with two silicene and one Ca atoms in a lateral 1 × 1 unit cell. The silicene layers possess alternately buckled Si atoms with rather large buckling amplitudes of 0.72 Å and 0.69 Å compared with 0.48 Å of freestanding silicene. For the Ca(111) substrate, a tensile strain acts on silicene, which results in a smaller buckling amplitude. For the functionalized Si substrate, no strain is present, so the larger buckling amplitude of 0.87 Å is a direct consequence of the interaction with the substrate. The Si atoms of silicene are placed on high-symmetry, threefold hollow sites of the uppermost Ca layer. The silicene–Ca layer distance of 2.0–2.1 Å is close to the distance of a Ca ML to the Si(111)1 × 1 substrate.

In the case of the silicene overlayers on Ca(0.5 ML) (figure 3(b)) and Ca(1.5 ML) (figure 3(d))-functionalized Si(111)2 × 1 surfaces, significant atomic rearrangements destroy the hexagonal symmetry of the silicene adsorbate layer. When comparing the clean Ca(0.5 ML)/Si (111) surface of figure 2 with silicene grown on the same surface in figure 3(b), an outward movement of the Ca atoms is visible. Two of the four silicene atoms per unit cell bind with the silicon atoms of the surface and are fourfold coordinated. This fact significantly modifies the interaction of silicene atoms with the Ca atoms. For 1.5 ML Ca coverage (figure 3(d)), a chain arrangement similar to the clean Ca(0.5 ML)/Si(111) surface is visible in figure 2. The silicene adapts to the surface features of the Ca-adsorbate layer. The 1.5 ML adsorbate of calcium decomposes into three Ca chains corresponding to 0.5 ML each. The lowest chain is similar to that found for the Ca(0.5 ML)/Si(111)2 × 1 surface. In the second Ca chain each atom occupies a fourfold-hollow site formed by two Ca and two Si atoms. In the third Ca chain the fourfold coordination is defined by one Ca and three Si atoms. The vertical distance of the second and third Ca chains is 1.15 Å. The atomic geometry of these two Ca chains determines the atomic arrangement of the silicene on top. The silicene overlayer also decays into two chains with a slightly larger vertical distance of 1.23 Å. Two of the four silicene atoms in a 2 × 1 unit cell are placed on a bridge site between two Ca atoms. The two other atoms occupy a threefold-hollow position formed by Ca atoms underneath, where the outward displaced silicene atom is surrounded by two lower and one upper Ca atoms and is laterally displaced towards the upper Ca. The other silicene atom is surrounded by one lower and two upper Ca atoms.

The relative stability of the silicene overlayers on different substrates is illustrated in the phase diagram versus the chemical potentials of Si and Ca in figure 4. The chemical potentials characterize the preparation conditions near thermal equilibrium. Only variations $\Delta\mu_X = \mu_X - \mu_X^{bulk}$ (X = Si, Ca) are studied with respect to the bulk values μ_X^{bulk} computed as

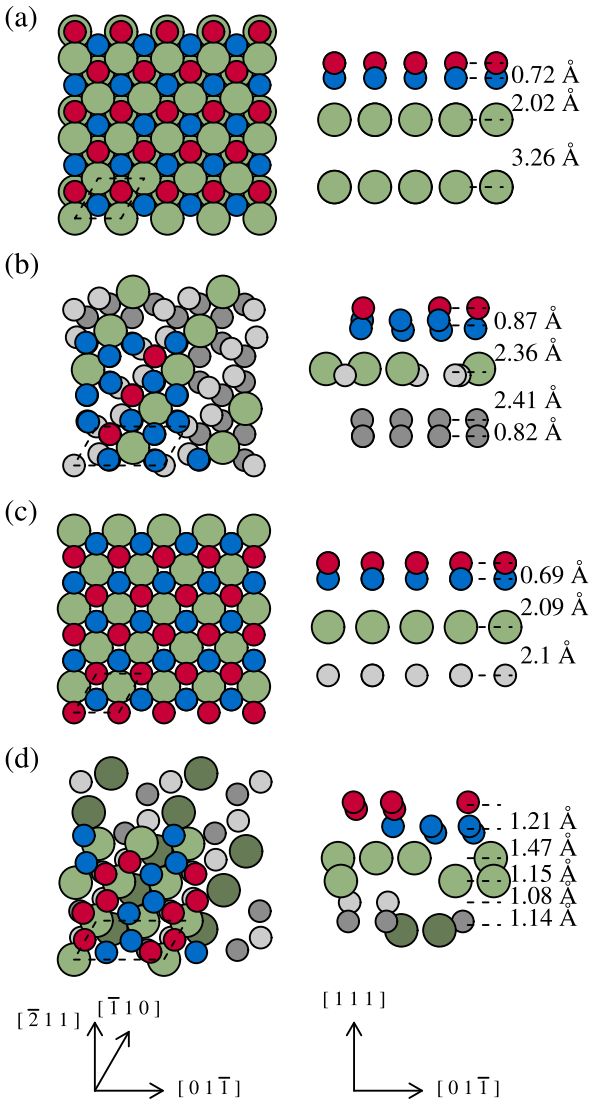

Figure 3. Top (left panels) and side (right panels) views of silicene on (a) Ca(111)1 × 1, (b) Ca(0.5ML)/Si(111)2 × 1, (c) Ca(1.0ML)/Si(111)1 × 1 and (d) Ca(1.5ML)/Si(111) 2 × 1 surfaces. The Ca (Si) atoms of the substrate are shown as green (grey) dots. The Si atoms of silicene are denoted by red (uppermost) or blue (lower) dots. The dashed lines illustrate the lateral surface unit cell. The numbers give the characteristic vertical distances.

the negative cohesive energy of diamond silicon and the fcc metal Ca. These values clearly represent X-rich preparation conditions. For comparison we use the formation energy of the silicene on top of clean Ca(111) or Ca-covered Si(111) surfaces,

$$\gamma = \frac{1}{2A}\left[E_{\text{slab}}\left(N_{\text{Si}}, N_{\text{Ca}}\right) - N_{\text{Si}}\mu_{\text{Si}} - N_{\text{Ca}}\mu_{\text{Ca}}\right]. \quad (1)$$

N_{Si} (N_{Ca}) is the number of Si (Ca) atoms in the slab system. A denotes the area of one slab surface, while the factor 2 is due to the use of symmetric slabs with two identical surfaces.

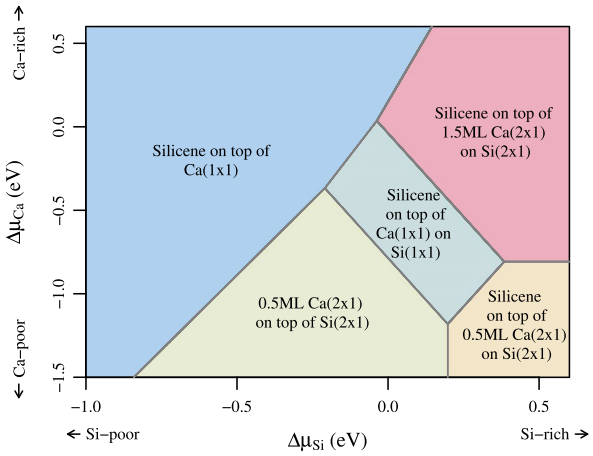

Figure 4. Phase diagram of silicene on four different surfaces and the Ca(0.5ML)/Si (111)2 × 1 substrate without silicene versus the chemical potentials of Si and Ca. The energy zeros correspond to the chemical potentials of bulk Si and Ca. The trends of preparation conditions are also indicated.

In the chosen intervals for $\Delta\mu_X$ four of the five studied silicene adsorbate geometries are stable. The silicene on Ca(1.0 ML)/Si(111)1 × 1 structure is energetically favored compared with the Ca(1.0 ML)/Si(111)2 × 1 reconstruction, which therefore does not appear in the phase diagram. The electronic structures are only discussed for the four metastable silicene geometries.

4.3. STM images

The filled- and empty-state STM images calculated for the four energetically favored adsorbate systems are displayed in figure 5. The perfect hexagonal honeycomb symmetry of the silicene overlayer on a clean Ca(111)1 × 1 surface (figure 5(a)) and a functionalized Ca(1.0 ML)/Si(111) 1 × 1 surface (figure 5(c)) is clearly demonstrated by the spot distributions. Similarly to silicene on Ag(111) the STM images are determined by the outermost silicene atoms [6–8, 11, 12, 32]. Also the filled- and empty-state images are rather similar; only the corrugation heights are different by a factor 2–3. These two images of silicene-covered Ca(111)1 × 1 and Ca(1.0 ML)/ Si(111)1 × 1 surfaces are close to those of freestanding silicene, and raise the hope to find the searched properties of silicene.

The situation is completely different for the other two images presented in figure 5. In figure 5(b), i.e., silicene on Ca(0.5 ML)/Si(111)2 × 1 substrate, the one outstanding silicene atom per unit cell is clearly visible in STM and forms a straight chain together with the outermost atoms of neighboring unit cells. Here a strong contrast between filled- and empty-state images exists. In figure 5(d), i.e., silicene on Ca(1.5 ML)/Si(111)2 × 1 substrate, the spots in the STM images are arranged in zig-zag chains due to the different heights of the silicene atoms, which are, nevertheless, arranged in hexagonal rings. This indicates completely different bonding behavior and a decay of the silicene layer into chain structures. The trenches, which are clearly visible between the zig-zag chains, are due to the fact that each second zig-zag chain is closer to the substrate and hence less visible in the STM image. The results presented in

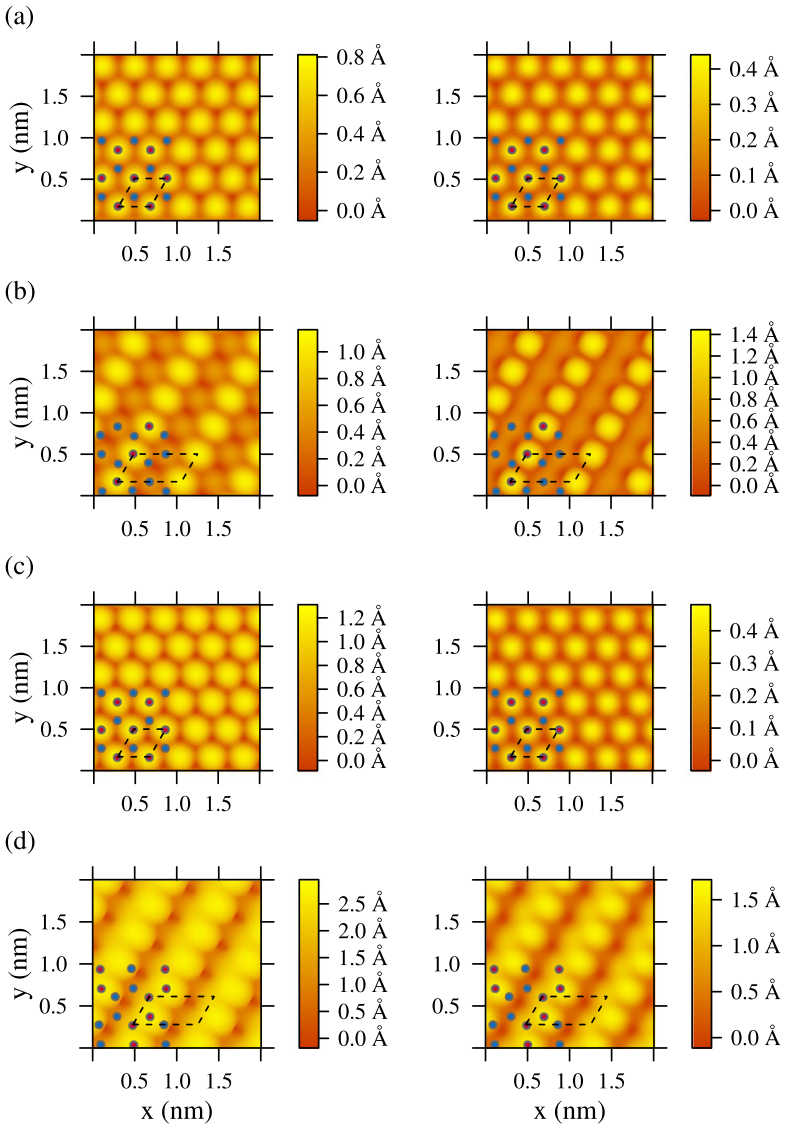

Figure 5. Filled-state (left) and empty-state (right) constant-current STM images for silicene on (a) Ca(111)1 × 1, (b) Ca(1.0ML)/Si(111)2 × 1, (c) Ca(1.0ML)/Si(111)1 × 1 and (d) Ca(1.5ML)/Si(111)2 × 1 surfaces. A bias voltage of ±1 V is applied. The positions of the silicene atoms are indicated by red (outermost atoms) and blue (lower atoms) dots.

figures 5(b) and (d) indicate that for the corresponding adsorbate systems the proof of evidence of silicene properties should be rather hopeless.

4.4. Band structures

The band structures versus the BZs in figure 6 of the four energetically favored silicene overlayers are presented in figure 7. The silicene p_z and p_{xy} projections are also given. At first glance, the four band structures look different. However, all investigated adsorbate systems are metallic. The Fermi level crosses several bands. Nevertheless, for the Ca(111)1 × 1 (a) and Ca

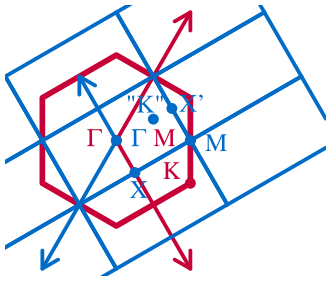

Figure 6. The two used 1 × 1 and 2 × 1 BZs are displayed. The reciprocal basis vectors are indicated by arrows. High-symmetry points of the hexagonal BZ and their projection onto the 2 × 1 rectangular BZ are denoted.

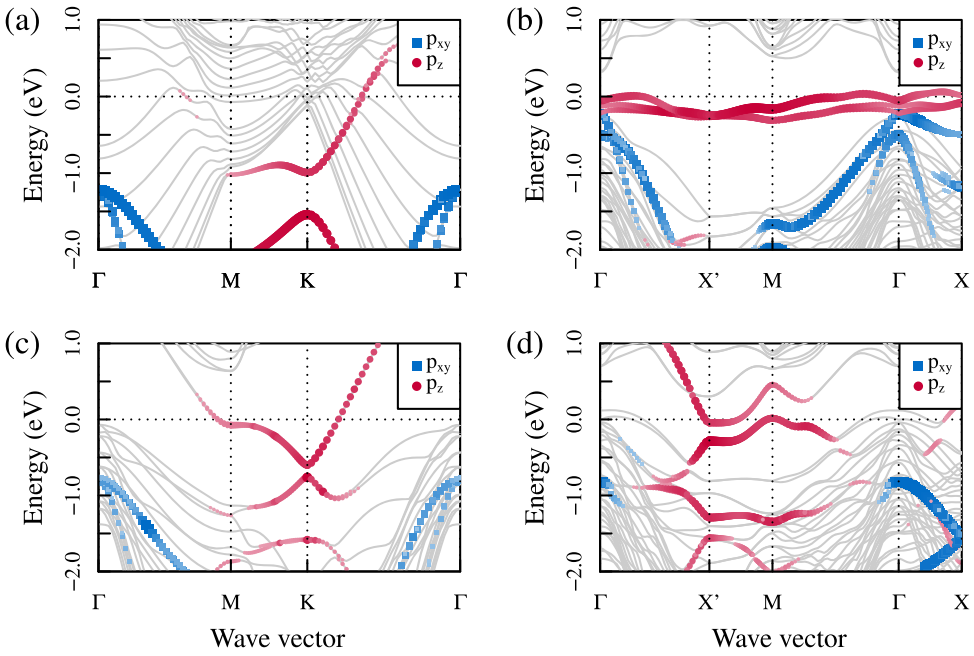

Figure 7. Band structures of silicene on (a) Ca(111)1 × 1, (b) Ca(0.5ML)/Si(111)2 × 1, (c) Ca(1.0ML)/Si(111)1 × 1 and (d) Ca(1.5ML)/Si(111)2 × 1 surfaces. The silicene p_z (silicene p_{xy}) character of the bands is indicated by red dots (blue squares) of varying size. All bands without silicene character are given by grey lines.

(1.0ML)/Si(111)1 × 1 (c) substrates Si p_z-state derived Dirac cones can be identified near the K point in the 1 × 1 BZ. However, there are some modifications: (i) the Dirac cones of the upper and lower bands are filled with electrons due to the metal substrate or the metallized Si(111) surface. (ii) Small gaps are opened between the Dirac cones near K. The two cones can be analytically described by

$$\varepsilon_{\pm}(\Delta\mathbf{k}) = \varepsilon_0 \pm \sqrt{\left(\frac{E_g}{2}\right)^2 + \left(\hbar v_{F\pm}\left|\Delta\mathbf{k}\right|\right)^2} \tag{2}$$

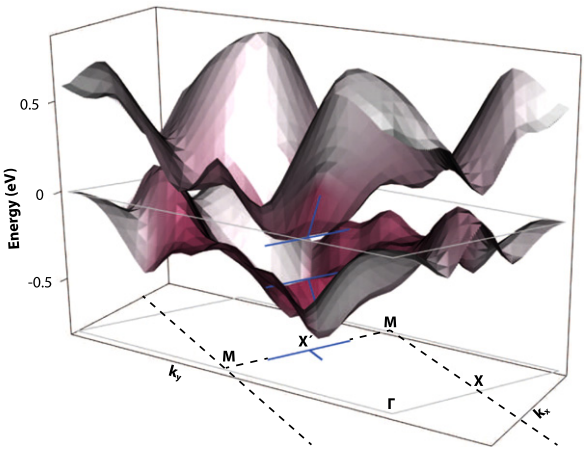

Figure 8. View of the two bands around the Fermi level, given as the energy zero, in the reciprocal space of the silicene on Ca(1.5ML)/Si(111)2 × 1 system. The strength of the silicene p_z character is indicated by the intensity of the red colour. The BZ is given by dashed lines. The positions of linear and vanishing dispersion are marked by blue lines.

for a **k** variation $\Delta\mathbf{k}$ around a K point. For silicene on the two substrates (a) and (c) in figure 7 we find gap openings of $E_g = 547$ and 161 meV. They indicate a stronger adsorbate-substrate interaction for the Ca(111)1 × 1 metal surface compared to the Ca(1.0 ML)/Si(111)1 × 1 one. In the case of Ca(1.0 ML)/Si(111)1 × 1 this interaction is reduced toward gap values that have been predicted for vdW bonding of silicene on passivated Si(111)1 × 1 surfaces [18]. The Fermi velocities are $v_{F+} = 0.38$ and 0.40×10^6 m s^{-1} or $v_{F-} = 0.44$ and 0.36×10^6 m s^{-1}. These values are only slightly smaller than the Fermi velocity of freestanding silicene.

In the case of the 2 × 1 translational symmetry in figure 7(b)/(d) for silicene on Ca(0.5 ML/1.5 ML) on Si(111)2 × 1, Dirac cones are difficult to identify. The K and K' points of the 1 × 1 BZ of silicene folded onto the 2 × 1 BZ of the adsorbate system, as illustrated in figure 6, the so-called *'K'* point, lies on the high-symmetry line ΓX′ in the smaller BZ. For Ca(0.5 ML)/Si(111) 2 × 1 very flat p_z-derived bands are equally distributed in the BZ. For Ca(1.5 ML)/Si(111)2 × 1, on the other hand, there is an indication for two linear bands 0.8 eV below the Fermi level. However, their silicene p_z-character, especially of the upper one, is small compared to the two bands closer to the Fermi level around a high-symmetry point X'. In order to make the shape of the p_z-derived bands clearer, the two uppermost bands near the Fermi level are plotted in figure 8 for **k** vectors in the reciprocal space. A linear band dispersion can be seen along the high-symmetry line ΓX′. Along the BZ boundary $X'M$, however, the band dispersion vanishes. The band shape could be described as a Dirac 'valley' instead of a Dirac cone.

5. Summary and conclusions

We have performed a screening of the (111) surfaces of fcc metals and (0001) surfaces of hexagonal metals in order to find appropriate substrates for silicene. Coincidence lattices were used to minimize strain in the epitaxial silicene. Apart from Ag(111) we found seven promising metal surfaces. However, after lattice relaxation only a silicene 1 × 1 overlayer on the Ca(111)

1 × 1 substrate still shows hexagonal symmetry and Dirac-cone-like features in the band structure.

Because of the promising results for clean Ca surfaces we have also investigated Si(111) surfaces functionalized by Ca atoms. Such substrates are lattice-matched to silicene, too. Because of the bivalent Ca atoms the most stable overlayer is a half Ca ML on a triple-bond Si (111)2 × 1 reconstruction with π-bonded Seiwatz chains. In addition, we have investigated coverages of 1 ML and 1.5 ML Ca atoms on Si(111) for possible deposition of silicene. The Ca (111)1 × 1 and Ca(1.0 ML)/Si(111)1 × 1 surfaces lead to silicene overlayers that exhibit conical linear bands near K and K' points but more than 0.5 eV below the Fermi level. The accompanying STM images clearly indicate honeycomb symmetry of the silicene overlayers. The Ca-functionalized Si(111)2 × 1 surfaces lead to the formation of chain motifs in the adsorbed silicene. Dirac-cone-like features are difficult to identify in the corresponding band structure for silicene on Ca(1.5 ML)/Si(111)2 × 1.

Acknowledgments

LM acknowledges financial support from the Carl-Zeiss Foundation.

References

[1] Durgun E, Tongay S and Ciraci S 2005 Silicon and III–V compound nanotubes: structural and electronic properties *Phys. Rev.* B **72** 075420
[2] Guzmán-Verri G G and Lew Yan Voon L C 2007 Electronic structure of silicon-based nanostructures *Phys. Rev.* B **76** 075131
[3] Cahangirov S, Topsakal M, Aktürk E, Şahin H and Ciraci S 2009 Two- and one-dimensional honeycomb structures of silicon and germanium *Phys. Rev. Lett.* **102** 236804
[4] Bechstedt F, Matthes L, Gori P and Pulci O 2012 Infrared absorbance of silicene and germanene *Appl. Phys. Lett.* **100** 261906
[5] Lalmi B, Oughaddou H, Enriquez H, Kara A, Vizzini S, Ealet B *et al* 2010 Epitaxial growth of a silicene sheet *Appl. Phys. Lett.* **97** 223109
[6] Vogt P *et al* 2012 Silicene: compelling experimental evidence for graphenelike two-dimensional silicon *Phys. Rev. Lett.* **108** 155501
[7] Lin C L *et al* 2012 Structure of silicene grown on Ag(111) *Appl. Phys. Express* **5** 045802
[8] Chen L *et al* 2012 Evidence for Dirac fermions in a honeycomb lattice based on silicon *Phys. Rev. Lett.* **109** 056804
[9] Meng L *et al* 2013 Buckled silicene formation on Ir(111) *Nano Lett.* **13** 685–90
[10] Fleurence A, Friedlein R, Ozaki T, Kawai H, Wang Y and Yamada-Takamura Y 2012 Experimental evidence for epitaxial silicene on diboride thin films *Phys. Rev. Lett.* **108** 245501
[11] Lin C L *et al* 2013 Substrate-induced symmetry breaking in silicene *Phys. Rev. Lett.* **110** 076801
[12] Arafune R, Lin C L, Nagao R, Kawai M and Takagi N 2013 Comment on 'Evidence for Dirac fermions in a honeycomb lattice based on silicon' *Phys. Rev. Lett.* **110** 229701
[13] Guo Z X, Furuya S, Iwata J I and Oshiyama A 2013 Absence of Dirac electrons in silicene on Ag(111) surfaces *J. Phys. Soc. Japan* **82** 063714
[14] Wang Y P and Cheng H P 2013 Absence of a Dirac cone in silicene on Ag(111): first-principles density functional calculations with a modified effective band structure technique *Phys. Rev.* B **87** 245430

[15] Gori P, Pulci O, Ronci F, Colonna S and Bechstedt F 2013 Origin of Dirac-cone-like features in silicon structures on Ag(111) and Ag(110) *J. Appl. Phys.* **114** 113710
[16] Cahangirov S *et al* 2013 Electronic structure of silicene on Ag(111): strong hybridization effects *Phys. Rev.* B **88** 035432
[17] Pflugradt P, Matthes L and Bechstedt F 2014 Unexpected symmetry and AA stacking of bilayer silicene on Ag(111) *Phys. Rev.* B **89** 205428
[18] Kokott S, Matthes L and Bechstedt F 2013 Silicene on hydrogen-passivated Si(111) and Ge(111) substrates *Phys. Status Solidi* **7** 538–41
[19] Liu H, Gao J and Zhao J 2013 Silicene on substrates: a way to preserve or tune its electronic properties *J. Phys. Chem.* C **117** 10353–9
[20] Gao N, Li J C and Jiang Q 2014 Bandgap opening in silicene: effect of substrates *Chem. Phys. Lett.* **592** 222–6
[21] Kresse G and Furthmüller J 1996 Efficient iterative schemes for *ab initio* total-energy calculations using a plane-wave basis set *Phys. Rev.* B **54** 11169–86
[22] Kresse G and Joubert D 1999 From ultrasoft pseudopotentials to the projector augmented-wave method *Phys. Rev.* B **59** 1758–75
[23] Dion M, Rydberg H, Schröder E, Langreth D C and Lundqvist B I 2004 Van der Waals density functional for general geometries *Phys. Rev. Lett.* **92** 246401
[24] Klimeš J, Bowler D R and Michaelides A 2011 Van der waals density functionals applied to solids *Phys. Rev.* B **83** 195131
[25] Monkhorst H J and Pack J D 1976 Special points for Brillouin-zone integrations *Phys. Rev.* B **13** 5188–92
[26] Kittel C 2005 *Introduction to Solid State Physics* 8th edn (New York: Wiley)
[27] Matthes L, Pulci O and Bechstedt F 2013 Massive Dirac quasiparticles in the optical absorbance of graphene, silicene, germanene and tinene *J. Phys.: Condens. Matter* **25** 395305
[28] Huang S, Kang W and Yang L 2013 Electronic structure and quasiparticle bandgap of silicene structures *Appl. Phys. Lett.* **102** 133106
[29] Rubloff G W 1983 Microscopic properties and behavior of silicide interfaces *Surf. Sci.* **132** 268–314
[30] Bechstedt F 2003 *Principles of Surface Physics* (Berlin: Springer)
[31] Kaloni T P, Cheng Y C and Schwingenschlögl U 2013 Hole doped Dirac states in silicene by biaxial tensile strain *J. Appl. Phys.* **113** 104305
[32] Pflugradt P, Matthes L and Bechstedt F 2014 Silicene-derived phases on Ag(111) substrate versus coverage: *ab initio* studies *Phys. Rev.* B **89** 035403
[33] Baski A A, Erwin S C, Turner M S, Jones K M, Dickinson J W and Carlisle J A 2001 Morphology and electronic structure of the Ca/Si(1 1 1) system *Surf. Sci.* **476** 22–34
[34] Sekiguchi T, Shimokoshi F, Nagao T and Hasegawa S 2001 A series of Ca-induced reconstructions on Si (111) surface *Surf. Sci.* **493** 148–56
[35] Sakamoto K, Takeyama W, Zhang H M and Uhrberg R I G 2002 Structural investigation of Ca/Si(111) surfaces *Phys. Rev.* B **66** 165319